Antarct. Meteorite Res., **16**, 13–33, 2003

Yamato nakhlites: Petrography and mineralogy

Naoya Imae[1], Yukio Ikeda[2], Keiji Shinoda[3], Hedeyasu Kojima[1] and Naoyoshi Iwata[4]

[1]*Antarctic Meteorites Research Center, National Institute of Polar Research, Kaga 1-chome, Itabashi-ku, Tokyo 173–8515*
[2]*Department of Material and Biological Sciences, Ibaraki University, Mito 310–8512*
[3]*Department of Geosciences, Faculty of Science, Osaka City University, 3–3–138, Sugimoto, Sumiyoshi-ku, Osaka 558–8585*
[4]*Faculty of Sciences, Yamagata University, 1–4–12, Kojirakawa, Yamagata 990–8560*

Abstract: We carried out the petrographical and mineralogical study of new Yamato nakhlites, Yamato 000593 (Y000593), Y000749 and Y000802, with electron probe microanalyzer and Fourier transform infrared microspectrometer. Euhedral pyroxenes ($En_{20-40}Fs_{22-40}Wo_{38-40}$) are the predominant phase with a modal proportion of 75–80 vol% and occur as elongated grains (~1 mm × 0.5 mm) with thin Fe-rich rims. The chemical composition of the augite cores comprising most of the volume of these pyroxene crystals is homogeneous and nearly identical with those in other nakhlites. Fe-rich rims are present in contact with the mesostasis. Anhedral ferroan olivines (Fa_{62-78}; 8–18 vol%, ~0.5 mm) and subhedral titanomagnetites (< 1 vol%, smaller than ~0.1 mm) are minor phenocrysts. The remainder of the meteoritic material is mesostasis (8–15 vol%), which predominantly consists of plagioclase ($An_{26-32}Ab_{63-65}Or_{4-8}$). Minor phases in the mesostasis are pyrrhotite ($Fe_{0.86-0.88}S$; smaller than 20 μm), apatite (smaller than 20 μm), titanomagnetite, Ca-poor pyroxene, fayalitic olivine ($Fa_{\sim 85}$), tridymite and iddingsite.

We distinguish these Yamato nakhlites from other nakhlites based on the chemical compositional ranges of the cores and rims of olivine and pyroxene phenocrysts. We suggest that the chemical variations of these minerals for the Yamato nakhlites are intermediate between those of NWA817 and others (Nakhla, Governador Valadares, and Lafayette).

The study by Fourier transform infrared microspectrometer of altered phases both on rims and fractures in olivine phenocrysts and in mesostasis revealed the existence of OH-bearing minerals, which might be mixtures of montmorillonite (70%) and goethite (30%). The existence of bubbles in an OH-bearing phase in olivine grains in contact with the fusion crust suggests that the alteration occurred before atmospheric entry (*i.e.* Martian origin).

key words: nakhlites, Martian meteorites, Y000593, Y000749, Y000802

1. Introduction

The nakhlites are one of igneous meteorites, and are part of the SNC (shergottites, nakhlites, and Chassigny) group based on oxygen isotopes (Clayton, 1993). Nakhlites are cumulus ultramafic rocks mainly consisting of clinopyroxenes (augites), and the bulk chemical composition is basaltic. SNCs may have come from Mars based on the

similarities of the rare gas data for SNCs with the data for Martian atmosphere measured by the Viking spacecraft(s) (McSween, 1985).

Until very recently, only three nakhlites (Nakhla, Lafayette, and Governador Valadares) were available for study. Recently, one nakhlite [Northwest Africa (NWA) 817] was recovered in a hot Saharan desert (Sautter *et al.*, 2002), and three nakhlites were found in a cold Antarctic desert (Y000593, Y000749 and Y000802; Yamato nakhlites in short). The Yamato nakhlites were found in late November to early December of 2000 by the 41st Japanese Antarctic Research Expedition (JARE-41: November 1999–March 2001) (Kojima and Imae, 2001; Imae *et al.*, 2002; Kojima *et al.*, 2002). Y000593 is the largest nakhlite documented so far.

Previous mineralogical and petrological studies of nakhlites have been carried out both from the viewpoint of the magmatic petrogenesis (*e.g.*, Treiman, 1986; Longhi and Pan, 1989; Treiman, 1990; Longhi, 1991; Harvey and McSween, 1992a; Harvey and McSween, 1992b; Friedman Lentz *et al.*, 1999; Mikouchi and Miyamoto, 2002; Sautter *et al.*, 2002) and from that of the secondary alteration, that is, the formation of hydrous minerals, carbonates and sulfates by weathering on the Martian surface (Gooding *et al.*, 1991; Treiman *et al.*, 1993). Compositional variations among olivines of all nakhlites have also been discussed and have been explained by differences in cooling rates that reflect the burial depths from the Martian surface (Harvey and McSween, 1992a; Friedman Lentz *et al.*, 1999; Mikouchi and Miyamoto, 2002; Sautter *et al.*, 2002).

In the present study, we describe mineralogical and petrographical features of constituent minerals in the Yamato nakhlites based on data acquired using electron probe microanalyzer and Fourier transform infrared microspectrometer. We compare the compositional ranges of pyroxene and olivine in the Yamato nakhlites with those in other nakhlites. In addition, we carried out a mineralogical study of altered phases (iddingsites) formed on Mars.

2. Experiments

Six polished thin sections of Y000593 (47 mm^2 for the subnumber 61, 62 mm^2 for 67-1, and 113 mm^2 for 63-2), Y000749 (60 mm^2 for 1-1 and 97 mm^2 for 1-3) and Y000802 (100 mm^2 for 20-1) (Fig. 1) were studied by a polarizing optical microscope using transmitted and reflected light and two electron probe microanalyzers (JXA-8800 at NIPR and JXA-733 at Ibaraki Univ.). Modal abundances of constituent minerals were determined by weighing by a micro-balance each area extracted from an enlarged photograph. H. Haramura determined the bulk major element compositions of Y000593,64 (2.180 g) and Y000749,47 (2.014 g) by standard wet chemical analysis method (Haramura *et al.*, 1983). Measurements by the Fourier transform infrared microspectrometer (Shimadzu FTIR 4200 and IR microscope IMS-1 with wire grid polarizer) were carried out on weathering products such as iddingsite on olivine rims and in olivine cracks. Polished thin sections of Y000593,57, Y000593,58 and Y000749,49 were removed from slide glass attached by PMC thermal wax (Struers) using acetone. The Fourier transform infrared microspectra of montmorillonite from Clay Spur, Wyoming, USA and goethite from Bisbee, Cochise County, Arizona, USA were independently measured using transmitted infrared light and were used for

comparison with similar spectra for weathering products in the Yamato nakhlites. Cr$K\alpha$ was used for obtaining the diffraction patterns of silica minerals with a Gandolfi camera.

3. Results

3.1. Bulk compositions

Bulk compositions of Y000593 and Y000749 are shown in Table 1 with literature references for the other nakhlites. The two Yamato nakhlites are similar in bulk composition to each other and the other nakhlites (Table 1), confirming their classification as nakhlites (Kojima and Imae, 2001). However, these meteorites have somewhat higher Al_2O_3 concentrations than other nakhlites (Table 1).

3.2. Petrography and mineralogy

The observations of polished thin sections of the three Yamato nakhlites by polarizing optical microscope show that they are unbrecciated cumulus igneous rocks and consist predominantly of elongated euhedral augite crystals (~1 mm × 0.5 mm) with mesostasis (Fig. 1a–c). Phenocrysts of olivine and titanomagnetite also occur. The mesostasis consists mainly of plagioclase with minor amounts of K-feldspar, titanomagnetite, augite, Ca-poor pyroxene, fayalitic olivine, pyrrhotite, apatite and a

Table 1. Bulk chemical composition of Yamato nakhlites (analyzed by H. Haramura) with other three nakhlites.

	Y000593,64	Y000749,47	Nakhla*1)	Nakhla*2)	Governador Valarades*3)	Lafayette*4) (Fusion crust)
SiO_2	47.93	48.77	48.96	48.24	49.52	46.9
TiO_2	0.47	0.46	0.38	0.29	0.35	0.33
Al_2O_3	1.91	2.01	1.74	1.45	1.74	1.55
Fe_2O_3	2.05	2.03	1.29	–	1.14	–
FeO	19.82	19.19	19.63	20.64	18.62	22.7
MnO	0.59	0.58	0.09	0.54	0.67	0.79
MgO	11.10	11.08	12.01	12.47	10.92	12.9
CaO	14.71	15.08	15.17	15.08	15.82	13.4
Na_2O	0.64	0.68	0.41	0.42	0.82	0.36
K_2O	0.18	0.16	0.14	0.10	0.43	0.09
H_2O (−)	0.05	0.00	0.06	–	–	–
H_2O (+)	0.0	0.0	–	–	–	–
P_2O_5	0.29	0.13	n.d.	0.12	–	–
Cr_2O_3	0.24	0.28	0.33	0.42	0.21	0.18
FeS	0.07	0.09	–	n.d.	–	–
Total	100.05	100.5	99.89	100.77	100.24	99.2

*1) requoted Prior (1912) from Bunch and Reid (1975)
*2) McCarthy *et al.* (1974)
*3) Burragato *et al.* (1975)
*4) Boctor *et al.* (1976)

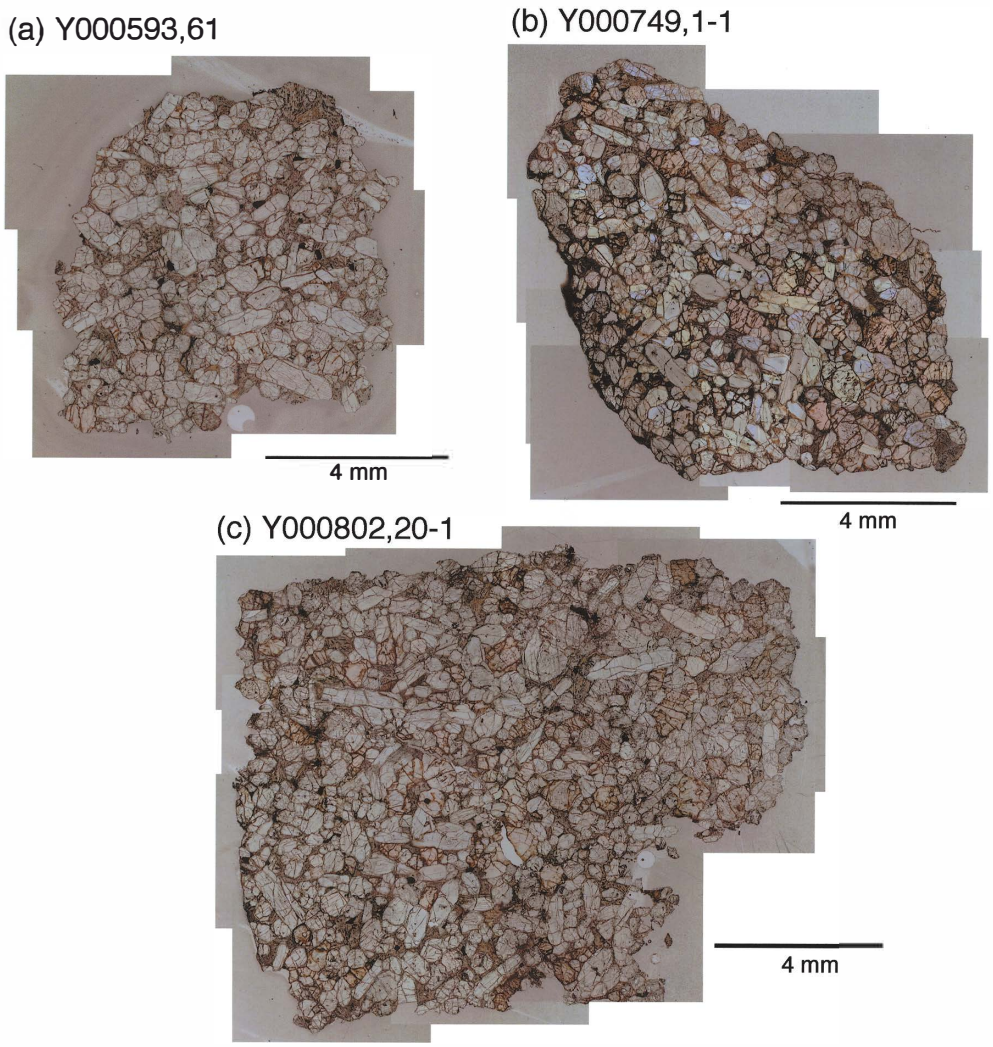

Fig. 1. (a)–(c) Polished thin sections (Y000593,61; Y000749,1-1; Y000802,20-1, respectively) under a polarizing optical microscope with transmitted light.

silica mineral. The silica mineral was identified as tridymite by the Gandolfi camera method. The overall textural features of the constituent minerals in the Yamato nakhlites are similar to those in Nakhla rather than those in Lafayette from the photographs of polished thin sections in Meyer (1998). This similarity is mainly due to the higher modal abundance of mesostasis of Yamato nakhlites and Nakhla than that of Lafayette. Chemical compositions of pyroxene, olivine, plagioclase and titanomagnetite are similar to those in other nakhlites.

Modal abundances of the constituent minerals (vol%) are summarized in Table 2. Olivine is more abundant in Y000749 and Y000802 than in Y000593. The abundance of mesostasis in the Yamato nakhlites is somewhat higher than that in Nakhla,

Table 2. Modal abundances (vol%) of main constituing minerals.

	Y 000593,64	Y000593,67-1	Y000749,47	Y000802,20-1	Yamato nakhlites (average)
Augite (phenocrysts)	75.6	84.2	70.7	76.2	76.7
Olivine (phenocrysts)	8.0	6.9	18.4	15.6	12.2
Titanomagnetite (phenocrysts)	1.0	0.6	0.3	0.5	0.6
Mesostasis	15.4	8.2	10.6	7.7	10.5
Pyrrhotite in mesostasis	<0.04				
Ca-apatite in mesostasis	<0.04				

	Nakhla[*1)]	Governador Valarades[*1)]	Lafayette[*1)]	NWA817[*2)]
Augite (phenocrysts)	79.9	79.3	74.5	69
Olivine (phenocrysts)	11.6	10.1	15.7	10
Titanomagnetite (phenocrysts)				1
Mesostasis	8.5	10.6	9.8	20

[*1)]Friedman Lentz *et al.* (1999)

[*2)]Sautter *et al.* (2002)

Governador Valadares, and Lafayette, which is supported by the somewhat higher Al_2O_3 concentrations in the bulk chemical analyses (Table 1).

3.2.1. Clinopyroxene phenocrysts

Euhedral pyroxene grains (Fig. 2a–c), which mostly consist of augite except for an outer rim of pigeonite, display pervasive polysynthetic twinning (Fig. 2c). Compositions of the phenocrystic augite cores are homogeneous ($En_{38-40}Fs_{24-26}Wo_{40-41}$) and the rims are Fe-rich (Fig. 3). The polysynthetic twinning may have been induced by shock metamorphism (Stöffler *et al.*, 1986). A few pyroxene phenocryst grains show undulatory extinction. Small inclusions (~1 μm) are abundant in many pyroxene grains though the phase, melt or fluid, has not been identified (Fig. 2b). Inclusions of titanomagnetite smaller than 5 μm in size are also found in some pyroxene phenocrysts.

The rims of augite phenocrysts in contact with the mesostasis (Fig. 2a) are 40–100 μm thick, and are ferrous up to ~Fs_{70} with a steep compositional slope (Fig. 4). The rims of augite phenocrysts in contact with another augite, olivine or titanomagnetite are not Fe-rich, and have similar composition with augite cores.

3.2.2. Olivine phenocrysts

Olivines (Fa_{58-83}; up to 0.5 mm in size) usually display a subhedral shape (Fig. 2d) and often include large augite inclusions (several tens of μm to 100 μm in size) (Fig. 2e). Many olivine crystals have symplectic exsolution lamellae (Fig. 2e and f). The

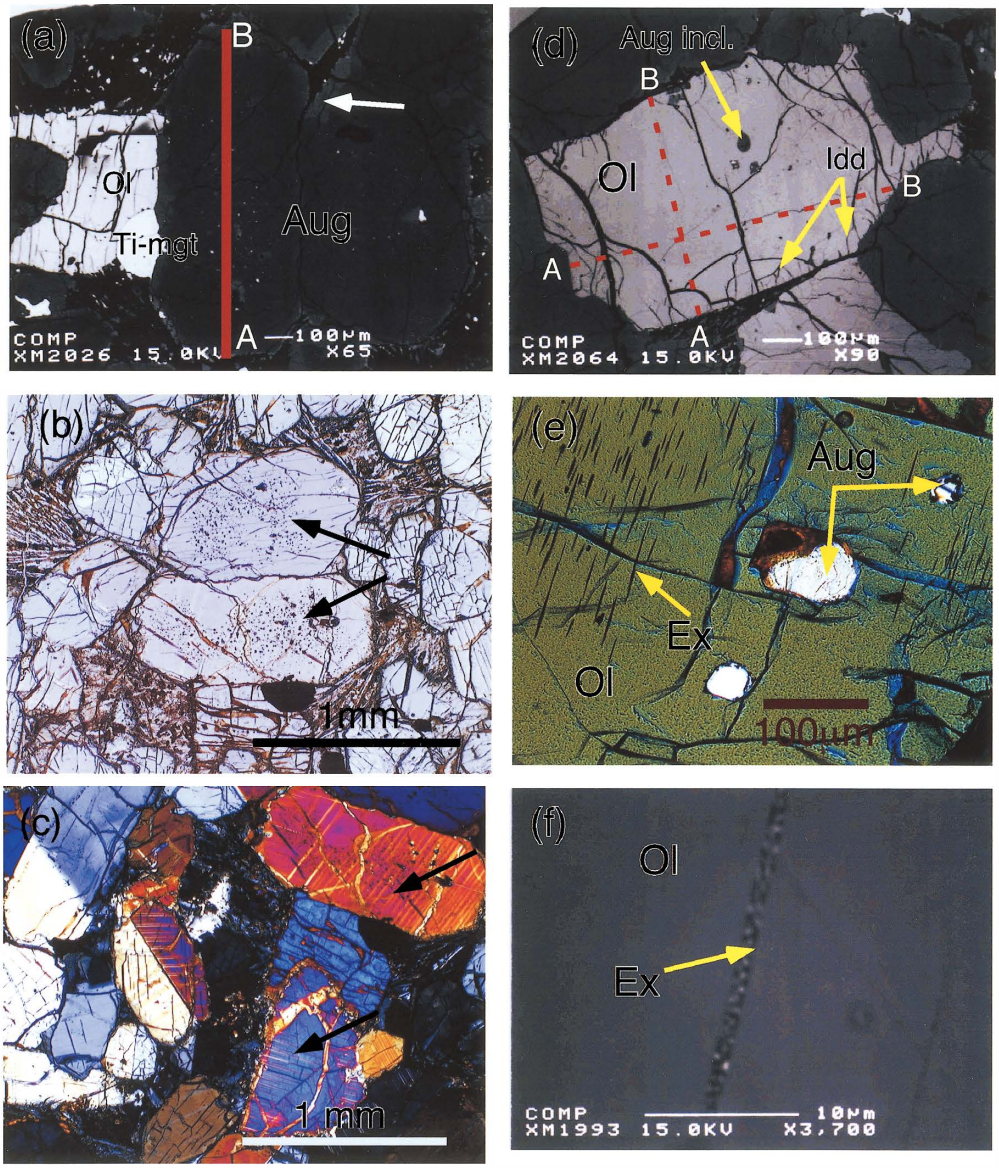

Fig. 2. Representative images in Y000593, Y000749 and Y000802. (a) Y000593,61. Back scattered electron image (BEI) of augite phenocrysts. A red line was examined for zoning profile in Fig. 4a. The overgrowth around augite core is shown as an arrow. Aug: augite. Ti-mgt: titanomagnetite. Ol: olivine. (b) Optical microscope image (OMI) with transmitted light of (a). Abundant fluid inclusion (arrows) can be observed in augite phenocrysts. (c) Y000593,61. OMI with cross nicols of augite phenocrysts showing polysynthetic twinning (arrows) of augites. (d) Y000593,61. BEI of an olivine phenocryst with a subhedral shape. Two dotted red lines were examined for zoning profiles in Fig. 6a.

An augite inclusion (Aug incl.) and iddingsite (Idd) are shown as arrows. Idd: iddingsite. (e) Y000593,61. Exsolution lamellae (Ex) in an olivine (OMI) and augite inclusions with crossed nichols.

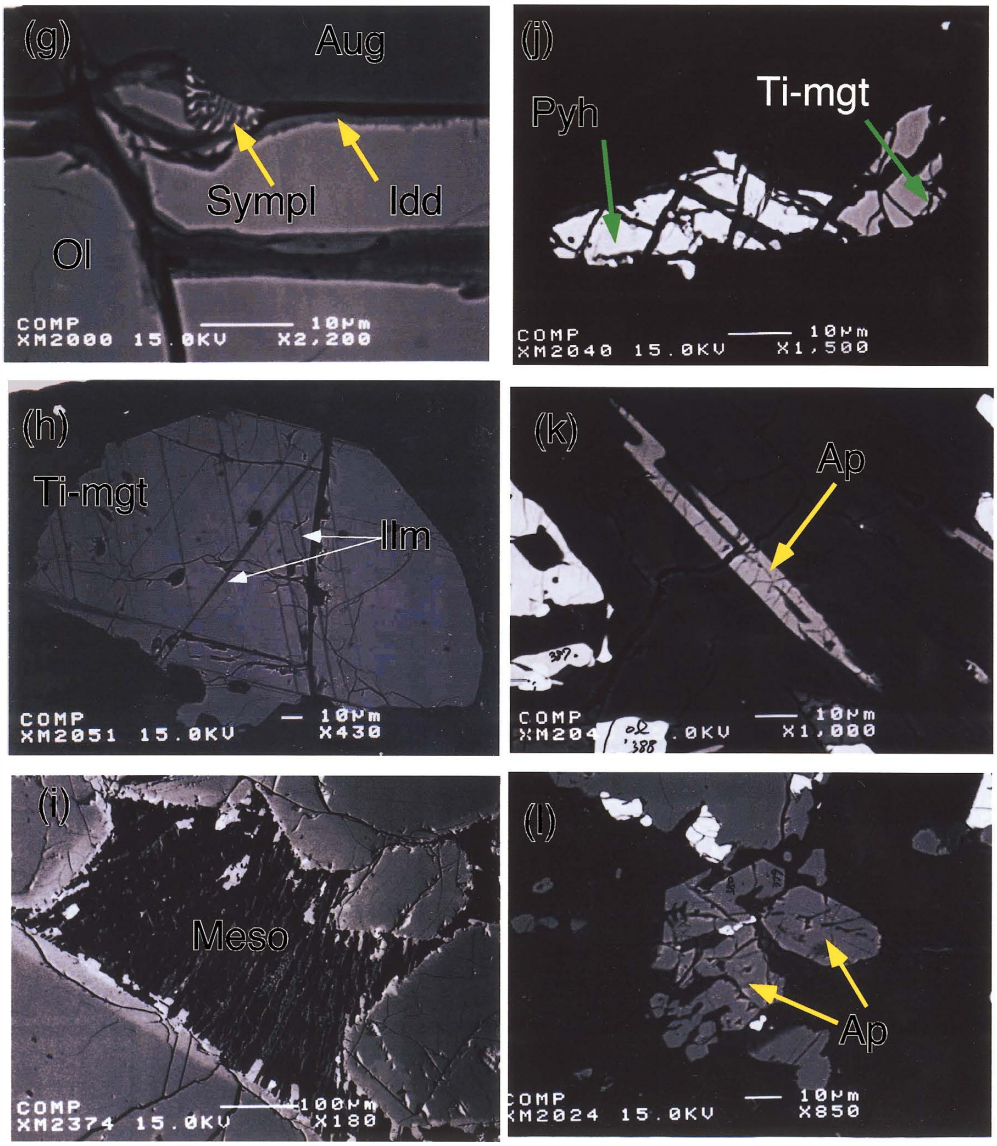

Fig. 2 (continued).

(f) Y000593,61. An enlarged BEI of exsolution lamellae in an olivine consisting of two phases. (g) Y000593,61. Symplectite (Sympl) in the interface between an olivine grain and an augite grain. Iddingsite (Idd) is also present in olivine. (h) Y000593,61. Titanomagnetite with ilmenite (Ilm) exsolution. (i) Y000802,20-1. Mesostasis (Meso) mainly consisting of plagioclase and pyroxene. In the mesostasis periphery, small titanomagnetite grains occur. (j) Y000593,61. Pyrrhotite (Pyh) and titanomagnetite in the mesostasis. (k) and (l) Y000593,61. Apatite (Ap) in the mesostasis.

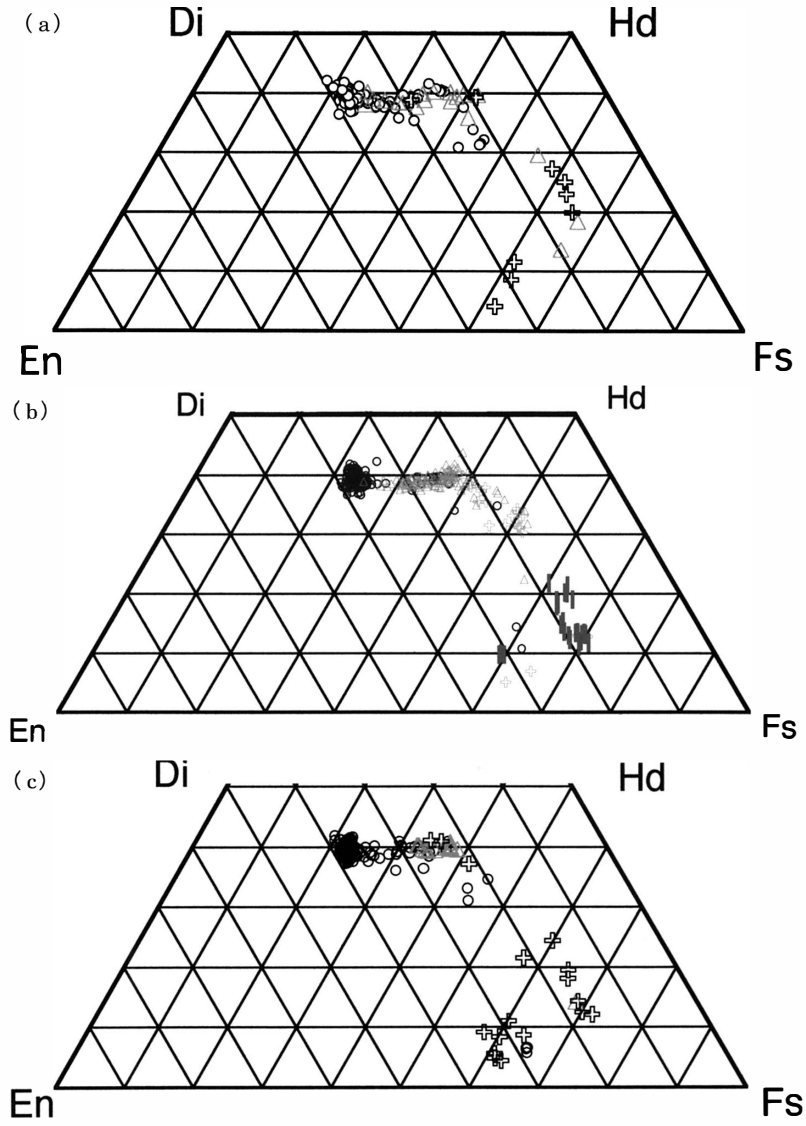

Fig. 3. Compositional variation of pyroxenes in three Yamato nakhlites. The compositions of the augite core are concentrated on the area of $En_{40\text{-}41}Fs_{20\text{-}21}Wo_{39\text{-}41}$. *Rims of augite grains are ferroan, resulting in chemical zoning in the rim region as shown in Fig. 4. The Wo content of the rim decreases outward through the constant Wo content, suggesting the formation of pigeonite. Most pyroxenes in the mesostasis are Ca-poor and they are subcalcic augite and pigeonite. (a) Open circle: phenocryst cores of augites (the number of analyses n=177). Open triangle: phenocryst rims of pyroxenes (n=21). Open cross: pyroxenes in the mesostasis (n=9). (b) Open circle: phenocryst cores of augites (the number of analyses n=224). Open triangle: phenocryst rims of pyroxenes (n=107). Open cross: pyroxenes in the mesostasis (n=22). Open triangle: pigeonites in the mesostasis (n=24). (c) Open circle: phenocryst cores of augites (the number of analyses n=183). Open triangle: phenocryst rims of pyroxenes (n=16). Open cross: pyroxenes in the mesostasis (n=18).*

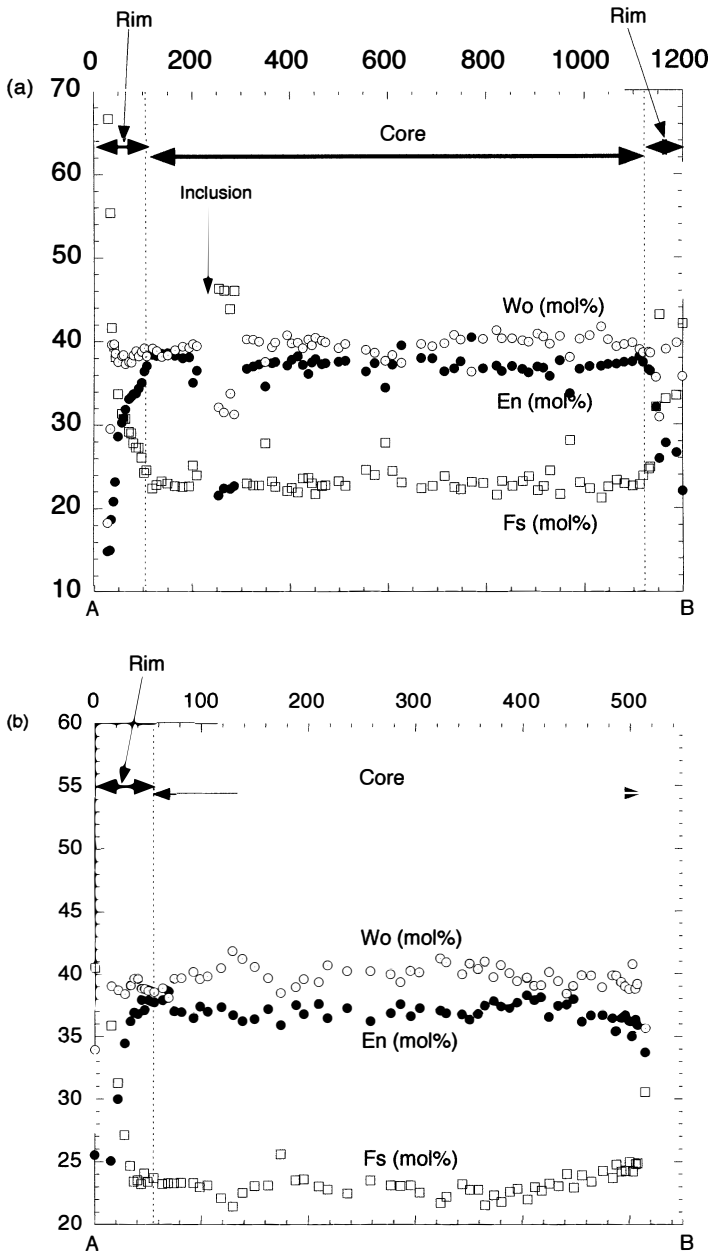

Fig. 4. Zoning profiles of a cummulus augite. (a) Y000593,61 left rim (A) with 105 μm thickness contacts with the mesostasis and the opposite right rim (B) of 80 μm thickness contacts with augite. The rim in contact with the mesostasis is Fe- and Al-richer than the rim contacting with augite. The discontinuity in Al_2O_3 in the rim is remarkable shown in the Al_2O_3 diagram. "Inclusion" shown in the figure represents titanomagnetite inclusion. (b) Y000749,1-1 left rim (A) with 55 μm thickness contacts with the mesostasis. On the other hand, overgrowth of the other side (B) contacting with augite that is not shown in this figure is not remarkable.

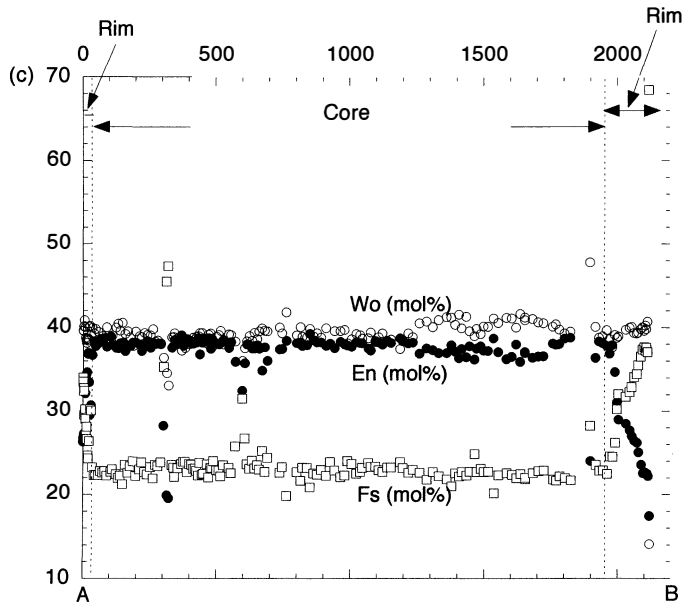

Fig. 4 (continued).
(c) Y000802,20-1. Both the left side rim (A) with 25 μm and the opposite rim (B) with 120 μm thickness contact with the mesostases.

lamellae are not homogeneously distributed within a host olivine (Fig. 2e). However, the lamellae have a preferred orientation in relation to the crystallographic axis of the host olivine, $<001>$ since the extinction orientation of the host olivine is parallel to the elongated direction of lamellae. These exsolution lamellae are commonly 30–40 μm in length and less than 2 μm in thickness. The lamellae have a symplectic texture consisting of two phases (Fig. 2f) and are similar to those in olivines from Nakhla (Mikouchi *et al.,* 2000) and Chassigny (Greshake *et al.,* 1998). According to Mikouchi *et al.* (2002), the two phases of lamellae in the Yamato nakhlites are magnetite and augite.

The symplectic structure is also found at the boundaries between olivine host and augite inclusions, and at the boundaries between olivine and augite phenocrysts (Fig. 2g).

Olivines have compositional ranges of Fa_{59-83} and 0.1–0.6 wt% of CaO for Y000593, Fa_{60-83} and 0.05–0.75 wt% of CaO for Y000749 and Fa_{58-77} and 0.05–0.95 wt% of CaO for Y000802 (Fig. 5). Zoning profiles of some olivine grains (Fig. 2d) are shown in Fig. 6. The cores are commonly more magnesian (Fa_{66-70}) than the rims (Fa_{74-78}). Abundance of CaO decreases from core (~0.5 wt%) to rim (0.02–0.3 wt%). As shown for Traverse 1 in Fig. 6(a), compositional zoning profiles of both Fa and CaO are not symmetrical. Steep zoning of Fa is shown especially on the side in contact with the mesostasis, whereas zoning of olivines in contact with augite is not steep (Fig. 6). Abundance of MnO is nearly constant at 1 wt%.

Rims and fractures in olivines are weathered (Fig. 2d and g). The weathered phase is apparently iddingsite by analogy with Nakhla (Gooding *et al.,* 1991). The

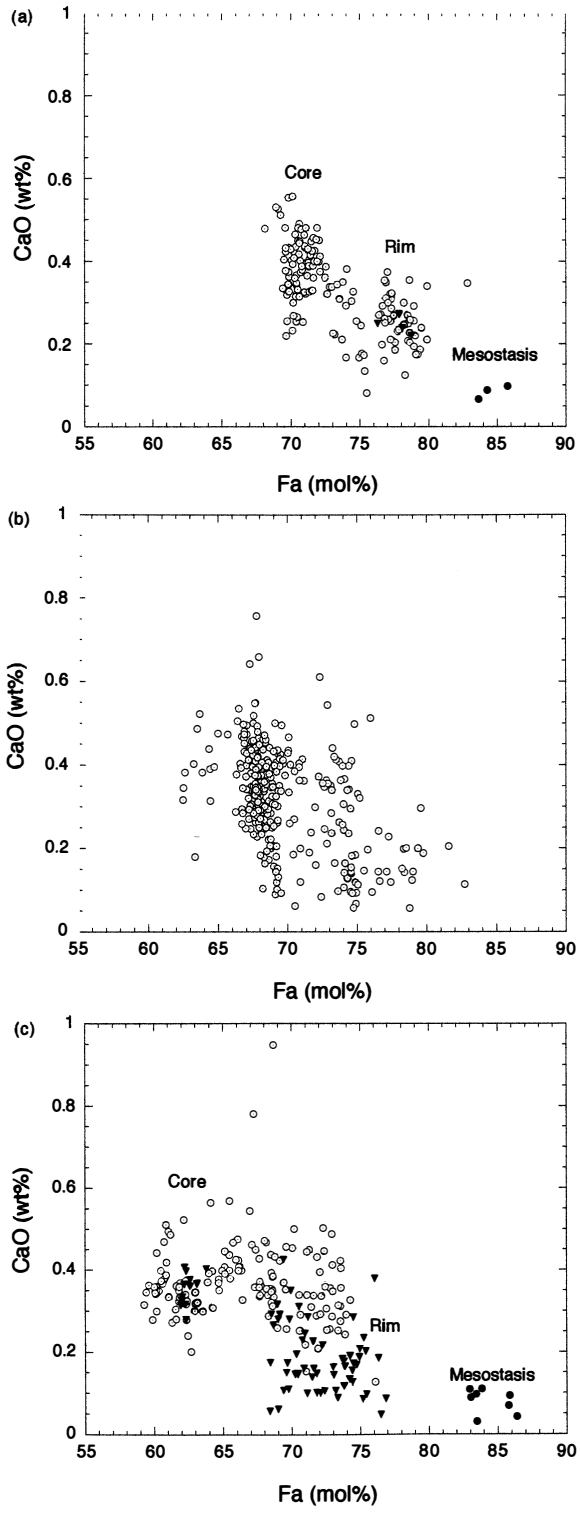

Fig. 5. (a)–(c) Compositional variation of olivines for three Yamato nakhlites. Dotted open circle: mostly core phenocryst olivines. Closed triangle: rims of phenocryst olivines. Closed circle: olivines in the mesostasis.
(a) Y000593,61.
(b) Y000749,1-1.
(c) Y000802,20-1.

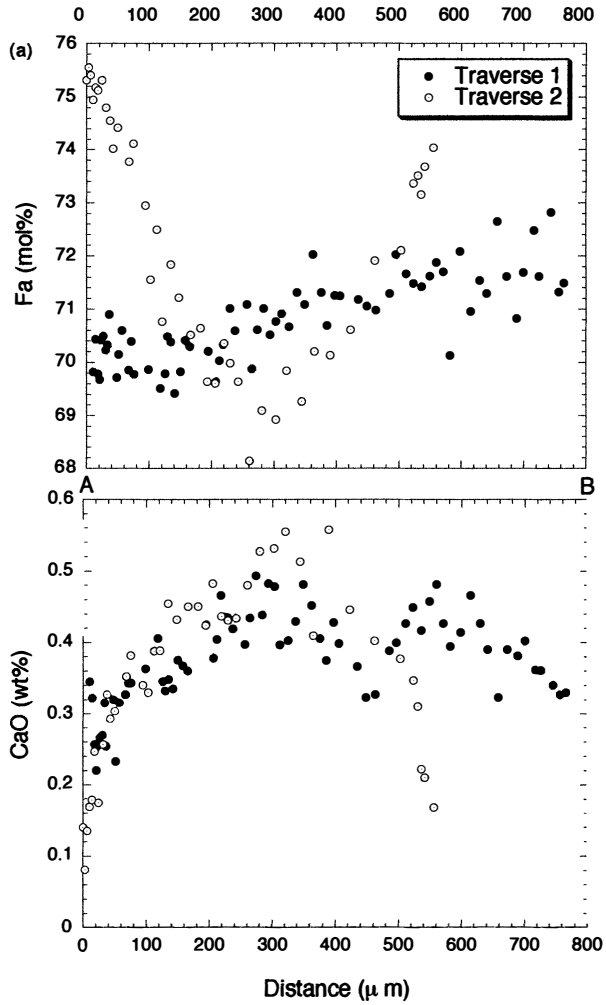

Fig. 6 a–c. Zoning profiles of olivine for three nakhlites. Fa (mol%) and CaO (wt%) content vs. distance (μm) are shown. Generally, Fa content in the rim contacting with the mesostasis is higher.
(a) Y000593,60. Traverse 1: The side "A" contacts with augite. The side "B" contacts with augite. Traverse 2: "A" contacts with the mesostasis. "B" contacts with augite.

spectra of the weathered phase in the Yamato nakhlites acquired by the Fourier transform infrared microspectrometer show a broad absorption peak in the range of 2800–3700 cm^{-1}, supporting the existence of iddingsite (Fig. 7). On the other hand, the absorption peak of hydrous minerals with high crystallinity such as serpentine, talc and brucite is sharp at 3692 cm^{-1} (*e.g.,* Shinoda and Aikawa, 1998; Imae *et al.,* 1999). Therefore, the observed spectra suggest substances with low crystallinity and are consistent with iddingsite. The broad absorption in Fig. 7 is also consistent with that of NWA817 (Gillet *et al.,* 2002).

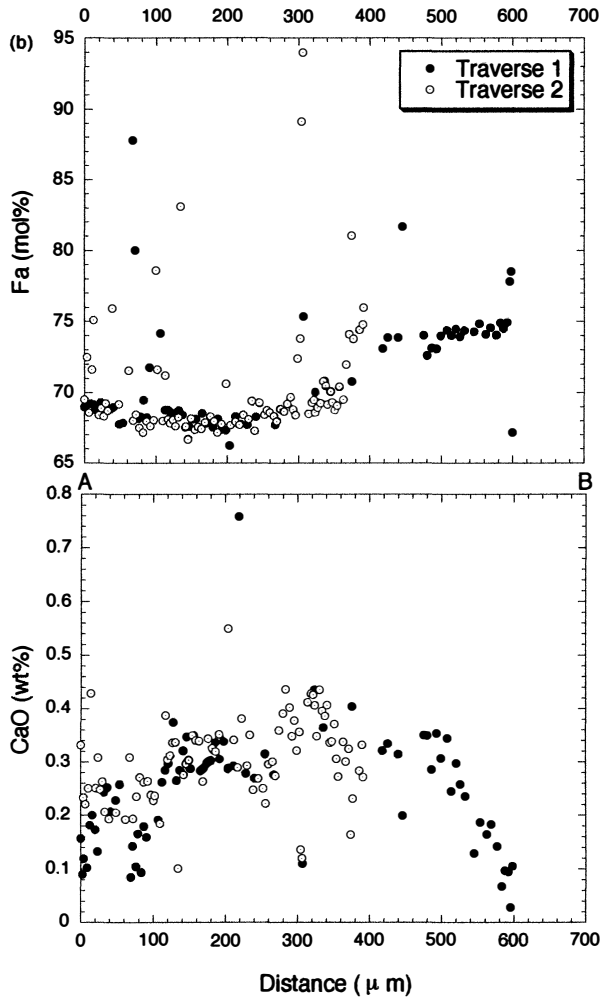

Fig. 6. (b) Y000749,1-1. Traverse 1: "A" contacts with augite. "B" contacts with the mesostasis. Traverse 2: "A" and "B" contact with augite.

3.2.3. Titanomagnetite phenocrysts

Subhedral to anhedral phenocrysts of titanomagnetite usually include ilmenite exsolution lamellae of ~10μm in width (Fig. 2h). This titanomagnetite is a two component mixture of magnetite and ulvöspinel; one is 32–68 mol% and the other varies in a complementary sense.

3.2.4. Mesostasis

The mesostasis consists predominantly of lath-shaped plagioclase (~10μm in width, $Ab_{60.3-68.1}An_{22.0-36.3}Or_{2.7-15.7}$) (Fig. 2i and Fig. 8). Minor phases include K-feldspar ($Ab_{33.9}An_{3.2}Or_{62.8}$; Fig. 8), augite, pigeonite, fayalitic olivine, titanomagnetite, pyrrhotite, apatite, tridymite and iddingsite. The composition of pigeonite in the

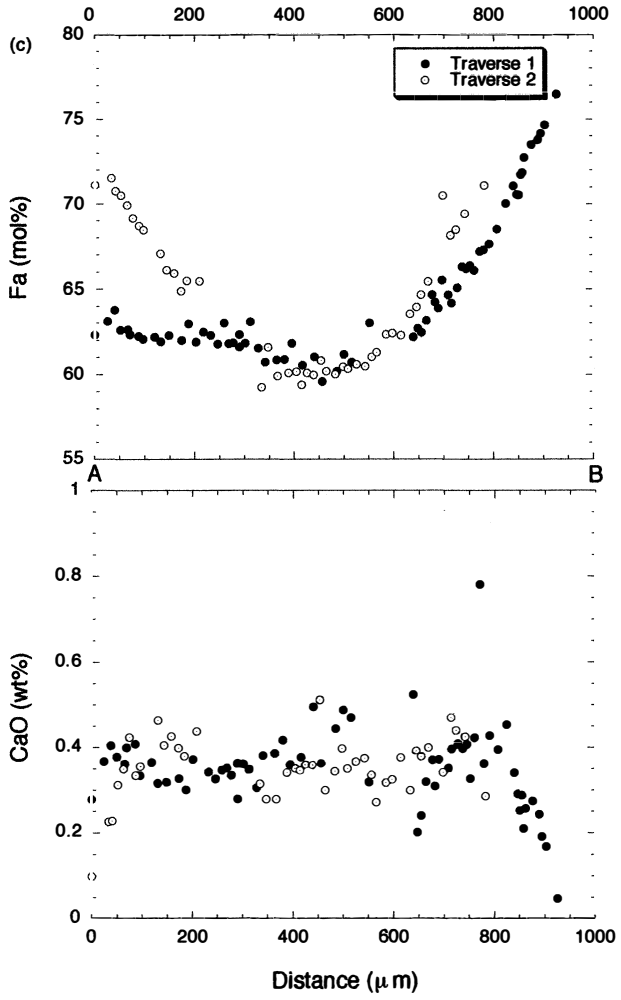

Fig. 6. (c) Y000802,20-1. Traverse 1: "A" contacts with augite. "B" contacts with the mesostasis. Traverse 2: "A" and "B" contact with the mesostases.

mesostasis overlaps with that of the outer rim of pyroxene phenocrysts, suggesting co-crystallization. Abundant small titanomagnetite grains, ~10μm in size (Fig. 2i), tend to occur in the periphery of mesostasis that is in contact with augite rims. Sulfides in Y000593 are pyrrhotite ($Fe_{0.86}S$-$Fe_{0.91}S$, Fig. 2j and Fig. 9). Apatites are rare, but occur as clusters of ~10μm sized grains with euhedral shape or as needle-like crystals (Fig. 2k and l). Mesostasis olivines are more ferroan ($Fa_{\sim 85}$) than phenocryst olivines. Altered phases in the mesostasis also show a broad absorption peak obtained by the Fourier transform infrared microspectrometer in a similar range as iddingsites in olivine, but the absorption degree is larger than that of iddingsites in olivines (Fig. 7).

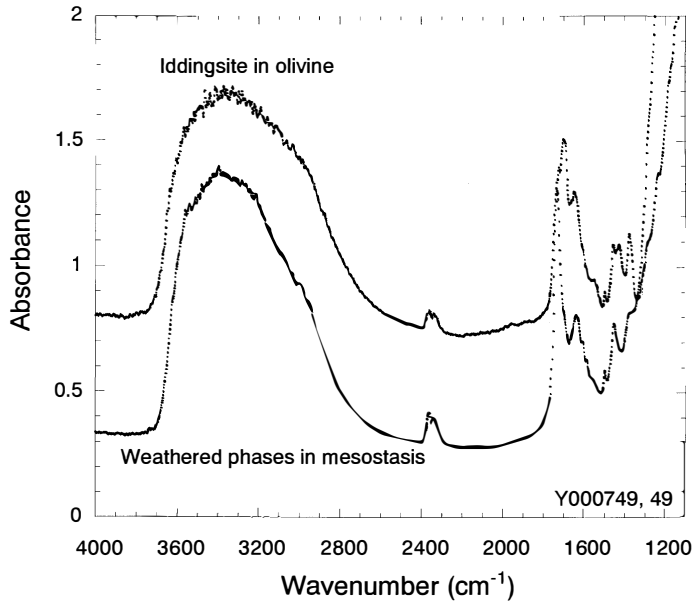

Fig. 7. The absorbance of weathered phases in Y000749,49 by Fourier transform infrared microspectrometer. A broad peak in the range of 3700–2800 cm^{-1} is observed for weathered phases (iddingsite) in olivines and mesostasis.

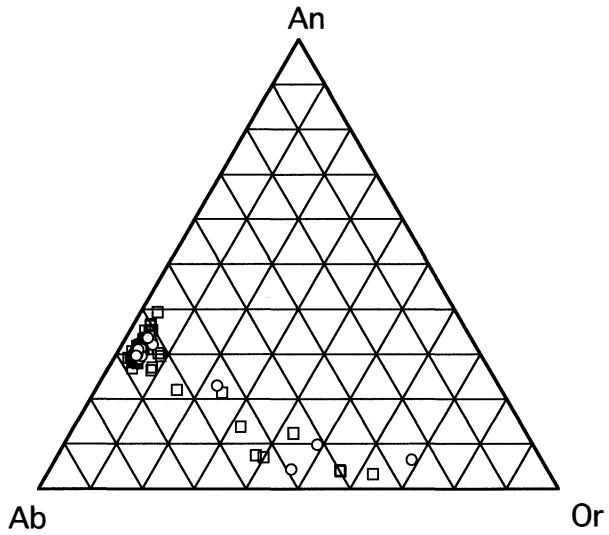

Fig. 8. The composition of feldspar in the mesostasis (open square: Y000593,61, open circle: Y000749,1-1). Or=$KAlSi_3O_8$, Ab=$NaAl_2Si_2O_8$, An=$CaAl_2Si_2O_8$.

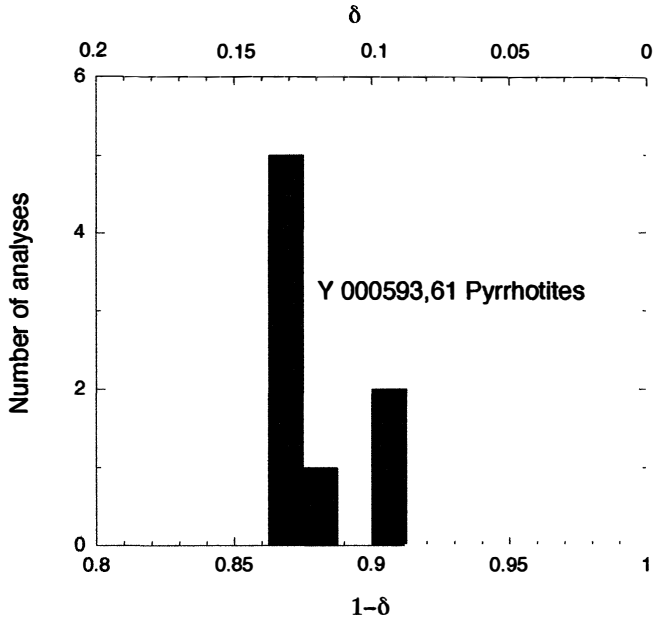

Fig. 9. Pyrrhotite chemical compositions in Y000593,61. Nonstoichiometry δ is in the range of 0.091–0.137.

4. Discussion

4.1. Comparison of nakhlites

4.1.1. Comparison between Yamato nakhlites

Table 1 indicates that the bulk compositions of Y000593 and Y000749 are nearly identical. However, the modal abundance of olivine is slightly different (Table 2): olivine tends to be greater in abundance in Y000749 and Y000802 than in Y000593. This difference in the olivine abundance may reflect local variations, as Nakhla shows heterogeneous olivine distribution (Mikouchi, private communication). Taking into account the close spacial occurrence in the field and the similar physical weathering degrees of these three Yamato nakhlites (Misawa *et al.,* 2003), we conclude that they are paired specimens. The rare gas data for these three Yamato nakhlites also support the pairing (Okazaki *et al.,* 2003).

4.1.2. Comparison of Yamato nakhlites with other nakhlites

Augite core compositions ($En_{36-39}Fs_{22-24}Wo_{38-41}$) for the Yamato nakhlites are similar to those ($En_{38-42}Fs_{22-25}Wo_{39-41}$) for Nakhla, Governador Valadares and Lafayette (Friedman Lentz *et al.,* 1999; Sautter *et al.,* 2002; Fig. 10).

The olivine phenocrysts of the Yamato nakhlites have a wider compositional range compared with those of other nakhlites (Friedman Lentz *et al.,* 1999; Sautter *et al.,* 2002). The compositional variation for the olivine phenocrysts of the Yamato nakhlites is similar to or slightly smaller than that of NWA817. From Fig. 10, the compositional variations of pyroxenes and olivines in Yamato nakhlites are intermediate

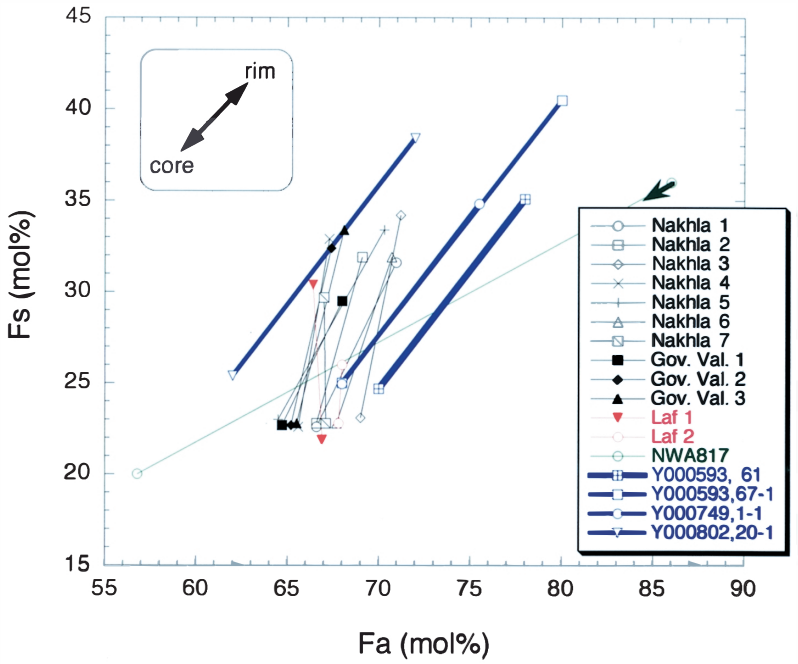

Fig. 10. Averaged core and rim compositional ranges of phenocrystic pyroxenes and phenocrystic olivines in nakhlites. A meteortie showing a wider compositional range of pyroxenes and olivines suggests that it has experienced more rapid cooling or lower annealing. The ferrosilite rim content is defined to be the averaged inner rim composition, under the condition that Wo content is constant. The data of Nakhla (1–7), Governador Valadares (Gov. Val. 1–3) and Lafayette (Laf 1–2) were taken from Friedman Lentz et al. (1999), where the sub-number means the different polished thin section. Data for NWA817 were taken from Sautter et al. (2002).

between those of NWA817 and others (Nakhla, Govenador Valadares and Lafayette).

Mikouchi and Miyamoto (2002) suggested that such variations of olivine compositions were the result of different burial depths on the parent body, that is, due to different cooling rates. When we consider that rims of augite phenocrysts formed after accumulation of core augites, the difference of the compositional ranges of the pyroxene could also be explained by the difference of the cooling rate of interstitial melt after accumulation of core augites; smaller compositional ranges indicate slower cooling, and larger ranges suggest more rapid cooling (Fig. 10).

4.2. Iddingsite formation

Iddingsite in olivine grains (Y000749,1-1) in contact with fusion crust contains abundant bubbles, suggesting decomposition of iddingsites by heating during atmospheric entry (Fig. 11a). This alteration texture, including bubbles in olivine grains near the fusion crust in Fig. 11a, is similar to that in Nakhla (Gooding *et al.,* 1991). This is textural evidence indicating that iddingsites dehydrated to form anhydrous minerals during atmospheric entry. Therefore, it is suggested that iddingsites had a pre-

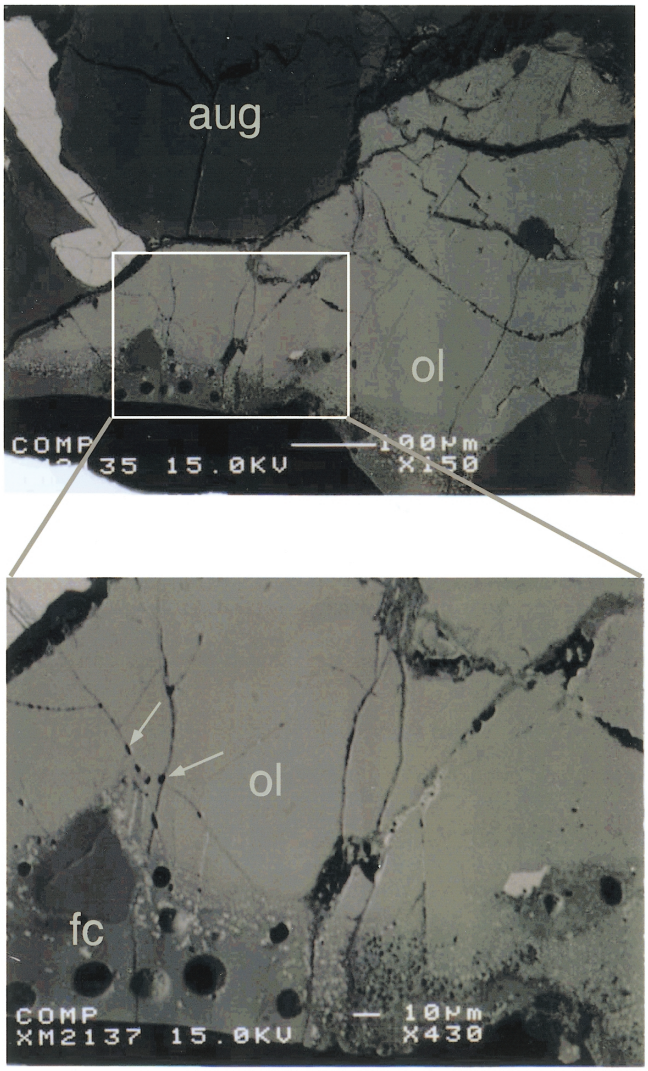

Fig. 11. (a) BEI of iddingsite that may have been formed before atmospheric entry. In fractures in an olivine grain in contact with fusion crust, abundant bubbles can be observed suggesting the decomposition of iddingsites by heating.

terrestrial origin. These iddingsites in the Yamato nakhlites formed on the parent body by the reaction of water liquid or water vapor with olivine as suggested by Gooding *et al.* (1991).

Iddingsite in nakhlites consists predominantly of mixtures of hydrous minerals probably including smectite (Gooding *et al.,* 1991), which is considered to have formed on the parent body (Mars surface) (Gooding *et al.,* 1991). The mechanical mixtures of I/I_0 by Fourier transform infrared microspectrometer under transmitted infrared light nearly reproduce the spectra of the corresponding natural mixtures (Prof. M.

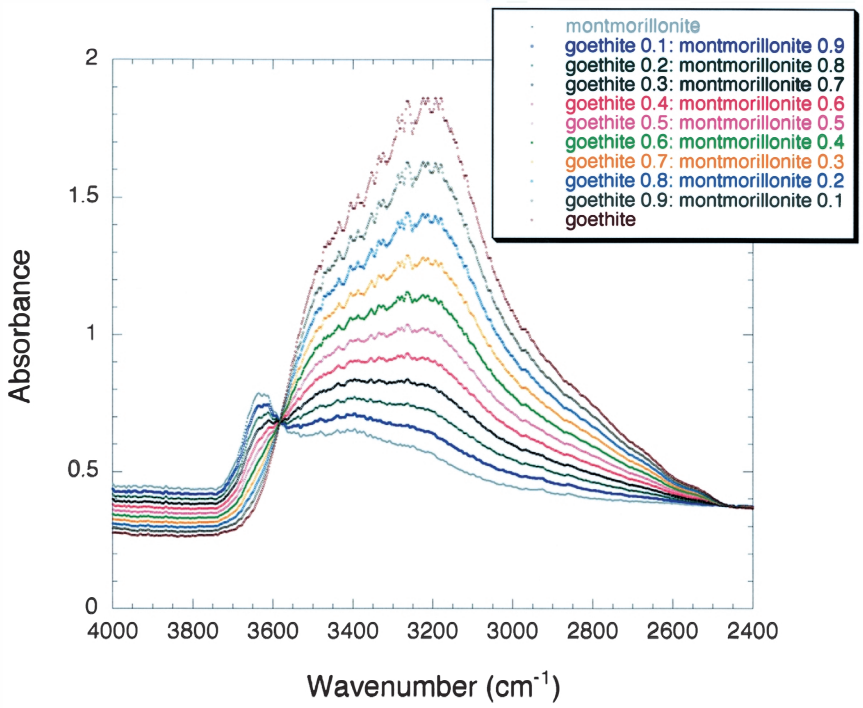

Fig. 11. (b) The absorbance of goethite, montmorillonite and the calculated mechanichal mixtures of goethite and montmorillonite. The mixture of 30% goethite and 70% montmorillonite is consistent with iddingsites in Yamato nakhlites in Fig. 7.

Miyamoto, personal comm.), where I is the intensity of the transmitted infrared light and I_0 initial intensity of the infrared light. Thus, we separately measured the absorption spectra of terrestrial goethite and montmorillonite and calculated the spectra of mechanical mixtures of various proportions of goethite and montmorillonite (Fig. 11b). We found that a mechanical mixture of 30% goethite and 70% montmorillonite (Fig. 11b) is most similar to the observation in Fig. 7. This suggests that iddingsite in the Yamato nakhlites consists mainly of goethite and montmorillonite.

5. Conclusions

(1) The three Yamato nakhlites, Y000593, Y000749 and Y000802, are paired.

(2) The averaged core–rim compositional ranges of pyroxene and olivine phenocrysts (*i.e.,* ferrosilite range and fayalite range, respectively) suggest that the Yamato nakhlites are an intermediate type between NWA817 and others (Nakhla, Governador Valadares and Lafayette) based on the chemical variation of pyroxenes and olivines.

(3) The study by the Fourier transform infrared microspectrometer shows that iddingsites in olivine fractures and in mesostasis mainly consist of goethite and montmorillonite. Iddingsites in olivines are probably of pre-terrestrial origin and

probably formed by Martian surface alteration.

Acknowledgments

We are grateful to the members of JARE-41 for support of the meteorite search in the Yamato bare ice region in Antarctica. The identification of a silica phase using Gandolfi camera was kindly carried out by Dr. Y. Nakamuta. We are grateful to Mr. H. Haramura for the bulk chemical analyses. We are also grateful to Drs. P. Buchanan, A. Yamaguchi, K. Misawa and H. Kaiden for reading the manuscript and grateful for the constructive review and discussions by Dr. T. Mikouchi and grateful to Dr. T. McCoy for a constructive review. The work is partially supported by Grant-in-Aid for Scientific Research from the Ministry of Education, Science, Sports and Culture of Japan (No. 13440168; P.I., K. Misawa).

References

Boctor, N.Z., Meyer, H.O.A. and Kullerud, G. (1976): Lafayette meteorite: Petrology and opaque mineralogy. Earth Planet. Sci. Lett., **32**, 69–76.

Bunch, T.E. and Reid, A.M. (1975): The nakhlites Part I: Petrography and mineral chemistry. Meteoritics, **10**, 303–315.

Burragato, F., Cavaretta, G. and Funiciello, R. (1975): The new Brazilian achondrite of Governador Valadares (Minas Gerais). Meteoritics, **10**, 374–375.

Clayton, R.N. (1993): Oxygen isotopes in meteorites. Ann. Rev. Earth Planet. Sci., **21**, 115–149.

Friedman Lentz, R.C., Taylor, G.J. and Treiman, A.H. (1999): Formation of a martian pyroxenite: A comparative study of the nakhlite meteorites and Theo's Flow. Meteorit. Planet. Sci., **34**, 919–932.

Gillet, Ph., Barrat, J.A., Deloule, E., Wadhwa, M., Jambon, A., Sautter, V., Devouard, B., Neuville, D., Benzerara, K. and Lesourd, M. (2002): Aqueous alteration in the Northwest Africa 817 (NWA817) Martian meteorite. Earth Planet. Sci. Lett., **203**, 431–444.

Gooding, J.L., Wentworth, S.J. and Zolensky, M.E. (1991): Aqueous alteration of the Nakhla meteorite. Meteoritics, **26**, 135–143.

Greshake, A., Stephen, T. and Rost, D. (1998): Symplectic exsolutions in olivine from the Martian meteorite Chassigny: Evidence for slow cooling under highly oxidizing conditions. Lunar and Planetary Science XXIX. Houston, Lunar Planet. Inst., Abstract #1069 (CD-ROM).

Haramura, H., Kushiro, I. and Yanai, K. (1983): Chemical compositions of Antarctic meteorites I. Mem. Natl Inst. Polar Res., Spec. Issue, **30**, 109–121.

Harvey, R.P. and McSween, H.Y., Jr. (1992a): Petrogenesis of the nakhlite meteorites: Evidence from cumulate mineral zoning. Geochim. Cosmochim. Acta, **56**, 1655–1663.

Harvey, R.P. and McSween, H.Y., Jr. (1992b): The parent magma of the nakhlite meteorites: Clues from melt inclusions. Earth Planet. Sci. Lett., **111**, 467–482.

Imae, N., Nakamuta, Y. and Shinoda, K. (1999): An experimental study of hydrous mineral formation by reaction between forsterite and water vapor. Proc. Japan Acad., **75**, Ser. B, No. 8, 229–234.

Imae, N., Okazaki, R., Kojima, H. and Nagao, K. (2002): The first nakhlite from Antarctica. Lunar and Planetary Science XXXIII. Houston, Lunar Planet. Inst., Abstract #1483 (CD-ROM).

Kojima, H. and Imae, N. (2001): Meteorite Newsletter, **10** (2), 9p.

Kojima, H., Nakamura, N., Imae, N. and Misawa, K. (2002): The Yamato nakhlite consortium. Antarctic Meteorites XXVII. Tokyo, Natl Inst. Polar Res., 66–68.

Longhi, J. (1991): Comparative liquidus equilibria of hyperthene-normative basalts at low pressure. Am. Mineral., **76**, 785–800.

Longhi, J. and Pan, V. (1989): The parent magmas of the SNC meteorites. Proc. Lunar Planet. Sci. Conf., 19th, 451–464.

McCarthy, T.S., Erlank, A.J., Willis, P. and Ahrens, L.H. (1974): New chemical analyses of six achondrites and one chondrite. Meteoritics, **9**, 215–221.

McSween, H.Y., Jr. (1985): SNC meteorites: Clues to Martian petrologic evolution? Rev. Geophys., **23**, 391–416.

Meyer, C. (1998): Mars Meteorite Compendium-1998. Houston, NASA.

Mikouchi, T., Yamada, I. and Miyamoto, M. (2000): Symplectic exsolution in olivine from the Nakhla martian meteorite. Meteorit. Planet. Sci., **35**, 937–942.

Mikouchi, T. and Miyamoto, M. (2002): Comparative cooling rates of nakhlites as inferred from iron-magnesium and calcium zoning of olivines. Lunar and Planetary Science XXXIII. Houston, Lunar Planet. Inst., Abstract #1343 (CD-ROM).

Mikouchi, T., Koizumi, E., Monkawa, A., Ueda, Y. and Miyamoto, M. (2002): Comparative mineralogy of the new nakhlite Yamato-000593 with other nakhlite Martian meteorites. Antarctic Meteorites XXVII. Tokyo, Natl Inst. Polar Res., 83–85.

Misawa, K., Kojima, H., Imae, N. and Nakamura, N. (2003): The Yamato nakhlite consortium. Antarct. Meteorite Res., **16**, 1–12.

Okazaki, R., Nagao, K., Imae, N. and Kojima, H. (2003): Noble gas signatures of Antarctic nakhlites, Yamato (Y) 000593, Y000749, and Y000802. Antarct. Meteorite Res., **16**, 58–79.

Prior, G.T. (1912): The meteoritic stones of El Nakhla El Baharia (Egypt). Mineral. Mag., **XVI**, 274–281.

Sautter, V., Barrat, J.A., Jambon, A., Lorand, J.P., Gillet, P., Javoy, M., Joron, J.L. and Lesourd, M. (2002): A new Martian meteorite from Morocco: the nakhlite North West Africa 817. Earth Planet. Sci. Lett., **195**, 223–238.

Shinoda, K. and Aikawa, N. (1998): Interlayer proton transfer in brucite under pressure by polarized IR spectroscopy to 5.3 GPa. Phys. Chem. Minerals, **25**, 197–202.

Stöffler, D., Ostertag, R., Jammes, C., Pfannschmidt, G., Sengupta, S.B., Simon, S.B., Papike, J.J. and Beauchamp, R.H. (1986): Shock metamorphism and petrography of the Shergotty achondrite. Geochim. Cosmochim. Acta, **50**, 889–903.

Treiman, A.H. (1986): The parental magma of the Nakhla achondrite: Ultrabasis volcanism on the shergottite parent body. Geochim. Cosmochim. Acta, **50**, 1061–1070.

Treiman, A.H. (1990): Complex petrogenesis of the Nakhla (SNC) meteorite: Evidence from petrography and mineral chemistry. Proc. Lunar Planet. Sci. Conf., 20th, 273–280.

Treiman, A.H., Barrett, R.A. and Gooding, J.L. (1993): Preterrestrial aqueous alteration of the Lafayette (SNC) meteorite. Meteoritics, **28**, 86–97.

(Received November 13, 2002; Revised manuscript accepted February 10, 2003)